



HAL
open science

Accurate analysis of the distribution of epicenters in Western Provence and Eastern Languedoc (Southern France)

Daniel Amorèse, Jean-Louis Lagarde, Emmanuel Baroux, Marianne Font, Jean-Paul Santoire

► **To cite this version:**

Daniel Amorèse, Jean-Louis Lagarde, Emmanuel Baroux, Marianne Font, Jean-Paul Santoire. Accurate analysis of the distribution of epicenters in Western Provence and Eastern Languedoc (Southern France). *Journal of Geodynamics*, 2008, 47 (1), pp.20. 10.1016/j.jog.2008.06.003 . hal-00531887

HAL Id: hal-00531887

<https://hal.science/hal-00531887>

Submitted on 4 Nov 2010

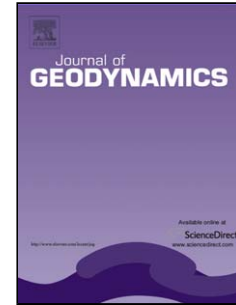
HAL is a multi-disciplinary open access archive for the deposit and dissemination of scientific research documents, whether they are published or not. The documents may come from teaching and research institutions in France or abroad, or from public or private research centers.

L'archive ouverte pluridisciplinaire **HAL**, est destinée au dépôt et à la diffusion de documents scientifiques de niveau recherche, publiés ou non, émanant des établissements d'enseignement et de recherche français ou étrangers, des laboratoires publics ou privés.

Accepted Manuscript

Title: Accurate analysis of the distribution of epicenters in Western Provence and Eastern Languedoc (Southern France)

Authors: Daniel Amorèse, Jean-Louis Lagarde, Emmanuel Baroux, Marianne Font, Jean-Paul Santoire



PII: S0264-3707(08)00045-8
DOI: doi:10.1016/j.jog.2008.06.003
Reference: GEOD 853

To appear in: *Journal of Geodynamics*

Received date: 29-12-2007
Revised date: 9-6-2008
Accepted date: 9-6-2008

Please cite this article as: Amorèse, D., Lagarde, J.-L., Baroux, E., Font, M., Santoire, J.-P., Accurate analysis of the distribution of epicenters in Western Provence and Eastern Languedoc (Southern France), *Journal of Geodynamics* (2007), doi:10.1016/j.jog.2008.06.003

This is a PDF file of an unedited manuscript that has been accepted for publication. As a service to our customers we are providing this early version of the manuscript. The manuscript will undergo copyediting, typesetting, and review of the resulting proof before it is published in its final form. Please note that during the production process errors may be discovered which could affect the content, and all legal disclaimers that apply to the journal pertain.

Accurate analysis of the distribution of epicenters in Western Provence and Eastern Languedoc (Southern France)

Daniel Amorèse^{a,*} Jean-Louis Lagarde^a Emmanuel Baroux^b
Marianne Font^a Jean-Paul Santoire^c

^a*Univ. Caen, F-14000 FRANCE ; CNRS, UMR 6143 M2C, Caen, F-14000
France*

^b*Istituto Nazionale di Geofisica e Vulcanologia, Via di Vigna Murata, 605, 00143
Roma, Italy*

^c*CEA-DASE-LDG, BP 12, 91680 Bruyères-le-Châtel, France*

Abstract

The present seismicity in Western Provence and Eastern Languedoc (Southern France) is weak. However, when the historical seismicity is considered, these regions are certainly among the most seismic areas of southern France. The tectonic setting of both regions is one of an active intraplate zone. In comparatively “stable” areas like these, the study of small instrumental earthquakes ($M < 5$) is an indispensable source of information. Unfortunately, in these regions, the instrumental seismicity is, as a rule, rare and diffuse. Therefore, interpreting the spatial pattern of this seismicity through a visual inspection is a difficult and subjective process. This paper presents a quantifiable analysis of the seismicity of the study regions. Earthquakes are associated with fault zones by examining the number of epicenters per unit area. The analysis is performed through the Blade method applied on collapsed

epicenters. The analyzed data are extracted from the Laboratoire de Détection et de Géophysique Catalog. Our analysis highlights several significant epicenter alignments associated with known tectonic features.

Key words: faults; earthquakes; epicenter alignments; France; Durance; Provence

PACS:

1 Introduction

2 The seismicity of southern France results from the conver-
3 gence between Africa and Europe. At present, Western Provence
4 and Eastern Languedoc are regions characterized by weak
5 seismicity (Fig. 1). A coarse calculation (from the Richards-
6 Dinger and Shearer's Catalog of seismicity (2000)) shows that
7 about 170 $M \geq 2$ seismic events occur in Southern California
8 per year and per 10^4 sq. km on average. For Western Provence
9 and Eastern Languedoc, this seismicity rate is less than 3
10 $M \geq 2$ events per year and per 10^4 sq. km. However, sev-
11 eral strong historical earthquakes (Fig. 1) have occurred in
12 the past in these regions (Lambert et al., 1996; Levret et al.,
13 1996). If we base the seismotectonic analysis on the histori-
14 cal seismicity, the study regions are certainly among the most
15 seismic areas of France : they include about 26 % of the known

* Corresponding author. Tel.: +33 231 565 719; fax: +33 231 565

757

Email address: daniel.amorese@unicaen.fr (Daniel

Amorèse).

16 damaging earthquakes of epicentral macroseismic intensity
17 degree $I_0 > VII$ (Lambert et al., 1996) but cover only about
18 18 % of the country's surface. This point is also supported by
19 indications of Quaternary deformation induced by destructive
20 earthquakes (Ghafiri, 1995; Sébrier et al., 1997). In this envi-
21 ronment, in terms of seismic hazard assessment, the identifi-
22 cation of the faults that have ruptured during these destruc-
23 tive events is of the utmost importance and is still under
24 debate (Cushing et al., 1997; Lacassin et al., 1998; Sébrier
25 et al., 1998; Baroux et al., 2003).

26 GPS quantification of the deformation in the study regions
27 or close to them (in the Southern Alps) shows that present
28 displacement rates are very small (Calais et al., 2000; Noc-
29 quet, 2002; Nocquet and Calais, 2004). Thus, the geodetic in-
30 formation seems to be consistent with the present day weak
31 seismicity. In such an environment, due to the absence of a
32 clear tectonic signal, the commonly used techniques for seis-
33 mic hazard assessment are not easily practicable. Despite the
34 difficulty, some of these techniques have been applied with
35 success in Provence (Carbon, 1996; Peulvast et al., 1999;
36 Schlupp et al., 2001; Baroux et al., 2001, 2003). It is never-
37 theless a fact that efforts should be taken to optimally use all
38 the available sources of information. In comparatively “sta-
39 ble” areas like these, the most conspicuous information con-
40 cerning active tectonics certainly comes from the study of
41 small earthquakes ($M < 5$) (Amorèse et al., 1999). Unfortu-
42 nately, in these regions, due to the “quiet” tectonic conditions

43 and/or the sparsity of the seismic networks, the instrumen-
44 tal seismicity is, as a rule, rare and diffuse. Thus, in “stable”
45 areas, analyzing the seismicity distribution and associating
46 earthquakes with faults are not straightforward processes.
47 This kind of analysis can be performed through mathemati-
48 cal methods. Nevertheless, until now, there have been no sys-
49 tematic (quantifiable) analysis of the distribution of the seis-
50 micity of Western Provence and Eastern Languedoc. Here, we
51 analyse the spatial distribution of the instrumental seismicity
52 and its relations with known faults or fault zones through the
53 mathematical approach of the Blade Method (Amorèse et al.,
54 1999). This method is applied on the instrumental seismic-
55 ity of the studied regions. As the seismicity of each of these
56 “relatively quiet” regions is sparse and diffuse, this kind of
57 mathematical analysis will fail to identify single seismogenic
58 faults. Nevertheless, this approach can help in the detection
59 of active fault zones. Moreover, through the Blade Method,
60 the “activity” of these fault zones can be somewhat quan-
61 tified. The Blade Method (Amorèse et al., 1999) has previ-
62 ously been applied with success both on epicentral data from
63 Normandy (Northwestern France) (Amorèse et al., 1999) and
64 Central United States (Amorèse, 2003). The method has been
65 tested on the seismicity of the San Francisco Bay area in
66 California (Amorèse et al., 1999). This is not a push-button
67 technique: the Blade Method is not self-sufficient. Because
68 random epicenter alignments are still possible, computations
69 issued from the Blade Method should be checked. Indeed, in

70 order to discard any false fault zone detection, the method
71 requires knowing the structural pattern of each study region.
72 This information is available: the structural pattern of East-
73 ern Provence and Western Languedoc has been well-known
74 for many years (Grellet et al., 1993).

75 **2 Tectonic setting**

76 The main geological structures of the study regions are due
77 to the two last tectonic events: the Pyrenean (Late Creta-
78 ceous to Late Eocene, about 70-40 Ma) and Alpine (Miocene
79 to present) tectonic phases. From West to East, three main
80 NNE-SSW faults are observed: the Cévennes, the Nîmes and
81 the Durance faults (Fig. 1). Another, smaller fault zone, is the
82 N-S Salon-Cavaillon fault system (Fig. 1). This smaller fault
83 is of special interest because it is known to have been active
84 during Quaternary times (Molliex et al., 2007). All these struc-
85 tures have been associated with the evolution of the passive
86 margin of the Tethys during the Early Jurassic. The study
87 regions are under a N-S compression (Combes, 1984; Rebai
88 et al., 1992; Baroux et al., 2001) and some evidence exists to
89 support the fact that the NNE-SSW and the E-W structures
90 are being reactivated by the present-day stress field (Dubois,
91 1966).
92 The Cévennes fault is a 180 km-long NE-SW striking fault
93 (Fig. 1). The possible activity of this structure (mainly in-

94 ferred from satellite images (Lacassin et al., 1998)) is clearly
95 debatable (Lacassin et al., 1998; Sébrier et al., 1998; Baize
96 et al., 2002).

97 Several authors consider the Nîmes fault as active (Combes
98 et al., 1993; Baroux, 2000). However, the activity of the Nîmes
99 fault is not unanimously accepted (Mattauer, 2002). Several
100 major historical earthquakes could be associated with the
101 Nîmes fault (Schlupp et al., 2001) : epicenters are mainly
102 located West of Avignon and in the Châteauneuf - du - Pape
103 area (Fig. 1). The Nîmes fault is extended in depth by a listric
104 fault dipping to the SE (Benedicto et al., 1996; Schlupp et al.,
105 2001). Its orientation (it strikes N50° and dips 60° southward)
106 is such that a N-S compression would appear to favor left-
107 lateral strike-slip motion with a possible reverse component
108 (Schlupp et al., 2001).

109 The Durance fault is considered as active by various authors
110 (Combes et al., 1993; Cushing et al., 1997; Baroux, 2000;
111 Cushing et al., 2007). The Durance fault is a sinistral strike-
112 slip fault (Combes et al., 1993) dipping to the NW. Although
113 the historical seismicity is regular in this area (on average, one
114 event of magnitude 5-5.5 per century (Volant et al., 2003)),
115 at present, the seismicity of the region of the Durance fault is
116 very low. Epicenters of historical earthquakes are mainly lo-
117 cated above the Manosque anticline (Peulvast et al., 1999). In
118 the Durance region, from North to South, several E-W com-
119 pressive fold zones may be possible sources of earthquakes.
120 These fold zones are : (1) the Mont Ventoux-Montagne de

121 Lure, (2) the Lubéron zone and (3) the Costes-Trévaresse fold
122 zones. The N110° Trévaresse thrust fault is responsible for the
123 June 11, 1909 Lambesc lethal earthquake (Levret et al., 1986;
124 Lacassin et al., 2001; Baroux et al., 2003).

125 The Salon-Cavaillon fault system (SCFS) is a 20-km long N-
126 S corridor where recent low deformation is suspected (Peul-
127 vast et al., 1999). It is proposed (Peulvast et al., 1999) that
128 subsidence occurs in the west, along the northern part of the
129 Salon-Cavaillon fault system. This subsidence could be partly
130 responsible for the diversion of the lower Durance towards the
131 Rhône river (Peulvast et al., 1999). Otherwise, uplift is well
132 known to occur along the 20-km long northern extension of
133 the SCFS (Fourniguet, 1987; Peulvast et al., 1999).

134 **3 Method**

135 Since years, many mathematical methods have been devel-
136 opped to associate seismicity with faults (Suzuki and Suzuki,
137 1965, 1966; Vere-Jones, 1978; Kagan and Knopoff, 1981; Fehler
138 et al., 1987; Frohlich and Davis, 1990; Tosi et al., 1994; Chap-
139 man et al., 1997; Amorèse et al., 1999; Gaillot et al., 2002;
140 Amorèse, 2003; Wesson et al., 2003). In this study, the seis-
141 micity of western Provence and eastern Languedoc is anal-
142 ysed through the Blade Method (Amorèse et al., 1999) com-
143 bined with an improved version of the Best Estimate Method
144 (Bossu, 2000). This new combined approach has previously

145 been applied with success on the seismicity of southern Illinois
146 and southeastern Missouri (Amorèse, 2003). Through this
147 kind of analysis based on instrumental seismicity, our purpose
148 is to highlight the most significant seismolineaments, indicat-
149 ing seismogenic structures. It is noteworthy that the Blade
150 Method does not include information from focal mechanisms
151 in the analysis. From this viewpoint, the Blade Method may
152 be less convincing than the method proposed by Chapman et
153 al. (1997) in their statistical analysis of the seismicity in the
154 Eastern Tennessee Seismic Zone. Unfortunately, in Western
155 Provence and Eastern Languedoc, very few well-constrained
156 focal mechanism solutions have been previously determined in
157 the vicinity of the known major tectonic features (Baroux et al., 2001).
158 Thus, in our study, focal mechanisms are not primary sources
159 of information and are only used to check our results. Here-
160 after, we present a summary of our methodology (for more de-
161 tails, refer to Amorèse et al (1999), Bossu (2000) and Amorèse
162 (2003)).
163 The Blade Method analyses the number of epicenters per unit
164 area. Each epicenter is the center of rotation of a blade (Fig.
165 2). The rotation of each blade is incremental. The value of
166 the angular increment depends on the desired angular reso-
167 lution and on the geometry (length, width) of the rotating
168 blade, in order to investigate the whole circular area. The
169 length of the blade controls the sensitivity of the method to
170 short- or long-range anisotropies in the point (epicenter) pat-
171 tern. Therefore, the choice of this value is dependent on the

172 lengths of the faults of the study zone (Fig. 3). The uncertain-
173 ties of the epicenter location are taken into account through
174 the width of the blades. The suitable value for the blade width
175 is about twice the mean uncertainty of the epicenter location
176 (Amorèse et al., 1999). For each blade position, the number of
177 observed points within the blade is determined and compared
178 with the number of points within the circular zone. Tests of
179 significance, based on binomial distributions, are performed.
180 The Blade Method is applied on epicentral locations: the as-
181 sociation of earthquakes with faults is based on the key as-
182 sumption that faults are steeply dipping faults or that seis-
183 micity is very shallow. This point is another argument to use
184 blades rather than lines in the detection process. The aim
185 of the Blade Method is not the detection of strictly linear
186 features because investigated points are supposed to be pro-
187 jected points from dipping fault planes, that, moreover, are
188 not necessarily strict planar structures.

189 Another difficulty arises from a possible inhomogeneous dis-
190 tribution of epicenters along each blade. In order to reduce
191 the influence of pointlike seismic nests, epicentral data anal-
192 ysed through the Blade Method should be previously filtered.
193 In this study, the filtering process is achieved through a epi-
194 center collapsing method: the Best Estimate Method (Bossu,
195 2000). Moreover, this approach reduces the effect of random
196 location uncertainties (Bossu, 2000). The procedure of the
197 Best Estimate Method is as follows (Bossu, 2000): a) for each
198 event i , the list of earthquakes whose initial locations fall

199 within its location uncertainty is determined; (b) the new
200 pseudo-location for i is then given by the centroid of all
201 these earthquakes; (c) steps (a) and (b) are repeated for all
202 hypocentres of the studied area. In this study, as in that by
203 Amorèse (2003), we do not use the original Best Estimate
204 Method, but a modified version of this technique. Indeed, the
205 original version of the Best Estimate Method is biased when
206 very badly located events are merged with well located events
207 (Amorèse, 2003). Once this filtering is done, the homogeneity
208 of the epicenter distribution along each blade is checked via
209 mean and standard deviation calculations. When mean and
210 standard deviation measurements of epicenter locations seem
211 not to be consistent with a uniform point distribution, the
212 corresponding blade is discarded (Amorèse et al., 1999).

213 The Blade Method is based on the hypothesis that, even dur-
214 ing the interseismic phase of the earthquake cycle, microseis-
215 micity, though weak, is not randomly distributed and is still
216 localized along major faults zones. It is not an obvious fact;
217 nevertheless the best example of this kind of seismic pattern
218 is certainly provided by the seismicity that occurred prior to
219 the $M_s=7.1$ Loma Prieta earthquake of October 17, 1989 in
220 California. The epicentral area of the mainshock was not a
221 microseism-free region before the earthquake occurrence (Fig.
222 4 and Dietz and Ellsworth (1997), Fig. 3). Thus, although
223 the Blade method cannot be successful in the detection of
224 perfectly locked (perfectly "aseismic") patches of faults, it
225 seems that it does not fail in the detection of possibly active

226 fault zones when the seismic activity is weak and diffuse. One
227 should bear in mind that the Blade method is a low resolu-
228 tion technique that cannot exactly identify active segments
229 of a given fault, if these segments are "short" and/or behave
230 in a perfectly "aseismic" manner.

231 4 Data and parameters of the computations

232 The area of investigation includes the western part of Provence
233 and eastern part of Languedoc between 43° N and 45° N and
234 1° E and 6.5° E (Fig. 1). The input data are 1634 epicenters
235 (magnitudes are ranging from $ML=1$ to $ML=5.3$) deter-
236 mined in this zone between 1962 and 2005 by the seismic
237 network of the Laboratoire de Détection et de Géophysique
238 (LDG/DASE/CEA). Superimposed onto background seismic-
239 ity, five large clusters are discernible in the Aubrac plateau,
240 near Montélimar city, in the Extern Alps (Haute Provence),
241 offshore east of Marseille and in the Espinouse mount (Fig.
242 1). From the 1634 events, 138 are discarded because they are
243 provided without ML magnitude information. Thus, what is
244 hereafter termed the 'raw data set' includes 1496 epicenters.
245 Data features and the best parameters for applying the Blade
246 Method are interdependent:

- 247 (1) The maximum uncertainty of epicenter location is the
248 value that controls the width of the rotating blades (Amorèse
249 et al., 1999; Amorèse, 2003).

250 (2) The length of the blades is controlled by the length dis-
251 tribution of the regional faults (Amorèse et al., 1999;
252 Amorèse, 2003).

253 In other respects, rotating blades are expected to show a
254 length-to-width ratio in agreement with the elongated map
255 view of a fault. When the Blade Method has been used in
256 previous studies (Amorèse et al., 1999; Amorèse, 2003), the
257 length-to-width ratio of the blades was always greater than
258 3:1.

259 In this study, in order to search for seismic features of differ-
260 ent lengths, the Blade Method has been applied twice. Once
261 the method has been performed by using (1) a 0.01 signifi-
262 cance level, (2) a 35 km long diameter for each circular zone,
263 (3) 12 km wide blades (this value is consistent with the 3:1
264 length-to-width ratio of rotating blades) and (4), in order to
265 offer a sufficient angular resolution, a 10° wide rotation an-
266 gular increment. This first application of the Blade Method
267 is in tune with the detection of the regional faults presented
268 in Figure 1, whose lengths are illustrated in Figure 3: the
269 blade length (35 km) is consistent with the mean value of the
270 lengths of the regional faults (32 km). Events with the major
271 axis of the 90 % confidence ellipse larger than 6 km are dis-
272 carded from our raw data set. Thus, 1011 event locations are
273 kept, which correspond to a 32 % reduction in the number of
274 events in the raw data set. Finally, from these 1011 events,
275 our modified version of the Best Estimate Method determines

276 873 pseudo-locations (Fig. 5).

277 The method is also performed by using a 70 km long diame-
278 ter (the other parameters being kept unchanged). In this case,
279 the search is for longer seismic features.

280 5 Results

281 In the study region, several seismolineaments are highlighed
282 by the combined use of the Best Estimate Method and Blade
283 Method. Results are presented in Figures 5 to 10 and Table
284 1. Our attention is first drawn to alignments in connection
285 with a previously recognized fault or fault zone.

286 In the Aubrac plateau area, no significant epicenter alignment
287 is detected (Fig. 6).

288 In the Montélimar area, the northern end of the Cévennes
289 fault is highlighted by the Blade Method as well as the N-S
290 Villefort fault (Figs. 7a and 7b). Illustrated by a smaller type
291 I error probability value (Table 1), the Villefort seismolinea-
292 ment is more clearly detected by a 35-km long blade than by
293 a 70-km long one. This is not true for the northern part of the
294 Cévennes fault: this seismolineament (North of the town of
295 Barjac, Fig. 7b) is better highlighted by the longer blade (the
296 p-value is $3.156 \cdot 10^{-6}$ for the 70-km long blade, Table 1). Close
297 to the town of Montélimar, the seismic area of Clansayes is
298 outlined by both instrumental and historical seismicity (Fig.
299 7a). However, no correlation is recognized between this seis-

300 micity and any mapped fault surface trace.

301 The Blade Method does not associate the Mont Ventoux-
302 Montagne de Lure, the Lubéron zone and the Costes fold
303 zone with any significant instrumental seismicity (Figs 8a
304 and 8b). On the contrary, the Durance Fault is clearly high-
305 lighted by N20° blades (Figs. 8a and 8b). This is especially
306 true for the southern blades that show the smallest values of
307 probabilities (Table 1). Moreover, the detected seismolinea-
308 ment coincides with the distribution of the historical macro-
309 seismic epicenters (Lambert et al., 1996) located near Volx,
310 Manosque, Beaumont-de-Pertuis and Mimet (Figs. 8a and
311 8b). Besides, this result is perfectly in agreement with the dis-
312 tribution of the seismicity located by the IRSN (Institute for
313 Radioprotection and Nuclear Safety) Durance local seismic
314 network (Cushing et al., 2007). Indeed, this study (Cushing
315 et al., 2007) shows an high density of earthquakes along the
316 N20° #9 fault segment (Cushing et al., 2007, Figure 5). In
317 the Durance Fault area, our results are also consistent with
318 the geometries of the fault-plane solutions that have been
319 determined by Volant et al (2000), close to the main fault
320 trace (Figs. 8a and 8b).

321 In the Salon-Cavaillon Fault System area (Fig. 9), the Nîmes
322 fault is not detected as a seismolinement by the Blade Method.
323 In this area, the only detected significant feature is the west-
324 ernmost N-S Salon-Cavaillon Fault (Fig. 9). The Blade Method
325 detects the seismolinement along the western edge of this
326 fault (Fig. 9). This is in agreement with the westerly dip of

327 the fault (Peulvast et al., 1999). The locations of historical
328 macroseismic epicenters near L'Isle-sur-la-Sorgue and Cavail-
329 lon (Lambert et al., 1996) are consistent with the result of
330 the Blade Method (Fig. 9).

331 In the Espinouse mount area, a N150° epicenter line is visi-
332 ble and detected near Corneilhan; nevertheless, as we argue
333 from our reference tectonic map, no significant seismolinea-
334 ment is detected (Fig. 10). In this area, as illustrated by the
335 rose diagrams (Fig. 10), blades tends to straddle faults that
336 are perpendicular to them.

337 **6 Conclusions**

338 Our results should be interpreted cautiously while bearing in
339 mind two intrinsic methodological limitations :

- 340 (1) The analysis is based on instrumental seismicity. It de-
341 pends on the capabilities of the recording seismic net-
342 work both in terms of detection thresholds and location
343 uncertainties. The spatial density of seismic stations is
344 the parameter controlling these points.
- 345 (2) The analysis depends on the relevancy of the tectonic
346 map that is used as the reference document.

347 Moreover, the spatial resolution is limited by the scale of
348 analysis. It depends on the lengths of blades and investi-
349 gated faults. In our analysis, small faults (cartographic length

350 shorter than 35 km) are underestimated as they are not con-
351 sidered as possible individual seismic sources. In spite of these
352 drawbacks, our study shows that, even when the seismicity is
353 poor, the spatial distribution of epicenters always carries use-
354 ful information. In our approach, the previously mentioned
355 influence of location uncertainties is weakened by considering
356 collapsed pseudo-locations instead of raw epicenter locations.
357 Despite the “bad” seismotectonic conditions of the study re-
358 gion, our analysis reveals that several known major tectonic
359 features in Western Provence and Eastern Languedoc can be
360 associated with a significant instrumental seismicity.

361 Of course, when it happens that instrumental seismicity is
362 not associated with a given fault by the Blade Method, this
363 does not mean that this fault is aseismic : in tectonic do-
364 mains where deformation rates are very small, the recurrence
365 interval of significant seismic events exceeds the time span
366 covered by instrumental records. Our analysis reveals that in
367 the Aubrac plateau area, in the Espinouse mount area or in
368 the Nîmes fault area, the instrumental seismicity seems to
369 be more randomly distributed than associated with a known
370 major fault.

371 On the contrary, the northern part of the Cévennes fault, the
372 Durance fault and the Salon-Cavaillon fault zone are marked
373 by epicenters whose alignments are statistically significant.
374 The Blade Method also highlights the Villefort fault. This re-
375 sult is unexpected because, due to the lack of a strong histor-
376 ical earthquake in its vicinity, this fault is usually not consid-

377 ered as an important structure in seismotectonic studies of
378 Provence. Our analysis suggests that thorough investigations
379 in the Villefort area might be fruitful in better estimating the
380 regional seismic hazard.

381 Our analysis is better than simply checking the instrumental
382 seismicity on each known tectonic feature, because it provides
383 quantitative values (the type I error probability values). Thus,
384 our procedure enables comparisons to be made within results.
385 It appears that the more convincing seismolineaments (i. e.
386 the seismolineaments that shows the smallest type I error p-
387 values) are associated with :

- 388 (1) the 70 km long Cévennes blade ($p = 3.156 \cdot 10^{-6}$)
- 389 (2) the 35 km long Durance southern blade, in the area of
390 Mimet ($p < 10^{-9}$)
- 391 (3) the 35 km long Villefort blade ($p = 2.945 \cdot 10^{-6}$).

392 Because the Blade Method does not give information on the
393 kinematics of faults, it is far beyond the scope of this study
394 to discuss the geodynamic setting of Western Provence and
395 Eastern Languedoc. Moreover, as accurately stated by Sébrier
396 et al. 1998, the correct assessment of the seismic hazard in a
397 weak deforming region implies a multidisciplinary approach.
398 Consequently, our study contributes to the understanding of
399 the seismotectonic conditions of Western Provence and East-
400 ern Languedoc, but it should be complemented by data from
401 other tectonic, geomorphological or geophysical studies to es-
402 tablish conclusive results about the regional seismic hazard.

403 **Acknowledgements**

404 Maps were prepared with the GMT software package (Wessel
405 and Smith, 1991). We acknowledge the Northern California
406 Earthquake Data Center and its contributors (the Northern
407 California Seismic Network of the U.S. Geological Survey at
408 Menlo Park and the Berkeley Seismological Laboratory of the
409 UC at Berkeley) for the epicentral data in Figure 4. We would
410 like to thank the editor and two anonymous referees for the
411 relevant and constructive reviews.

412 **References**

- 413 Amorèse, D., 2003. A new approach for associating earth-
414 quakes with geological structures: application to epicenters
415 in southern Illinois and southeastern Missouri. *Geophys.*
416 *Res. Lett.*, 30. Doi:10.1029/2003GL017247.
- 417 Amorèse, D., Lagarde, J.L., Laville, E., 1999. A point pattern
418 analysis of the distribution of earthquakes in Normandy
419 (France). *Bull. seism. Soc. Am.*, 89, 742–749.
- 420 Baize, S., Cushing, M., Lemeille, F., Granier, T., Grellet, B.,
421 Carbon, D., Combes, P., Hibsich, C., 2002. Inventaire de
422 indices de rupture affectant le Quaternaire, en relation avec
423 les grandes structures connues, en France métropolitaine et
424 dans les régions limitrophes. *Mém. Soc. géol. Fr.*, 175, 142
425 pp.
- 426 Baroux, E., 2000. Tectonique active en région à sismicité

- 427 modérée: le cas de la Provence (France). Apport d'une ap-
428 proche pluridisciplinaire. Ph.D. Thesis, University Paris
429 XI, Orsay, 327 pp.
- 430 Baroux, E., Béthoux, N., Bellier, O., 2001. Analyses of the
431 stress field in southeastern France from earthquake focal
432 mechanisms. *Geophys. J. Int.*, 145, 336.
- 433 Baroux, E., Pino, N.A., Valensise, G., Scotti, O., Cush-
434 ing, M.E., 2003. Source parameters of the 11 June
435 1909, Lambesc (Provence, southeastern France) earth-
436 quake: A reappraisal based on macroseismic, seismolog-
437 ical, and geodetic observations. *J. Geophys. Res.*, 108.
438 Doi:10.1029/2002JB002348.
- 439 Benedicto, E., Labaume, P., Séguret, M., Séranne, M., 1996.
440 Low-angle crustal ramp and basin geometry in the Gulf
441 of Lion passive margin: Oligocene-Aquitainian Vistrenque
442 graben, SE France. *Tectonics*, 15, 1192–1212.
- 443 Bossu, R., 2000. A simple approach to constrain the position
444 and the geometry of seismogenic structures: Application
445 to the Karthala volcano (Grande Comores Island, Mozam-
446 bique Channel). *Journal of Seismology*, 4, 41–48.
- 447 Calais, E., Galisson, L., Stéphan, J.F., Delteil, J., Deverchère,
448 J., Larroque, C., de Lépinay, B.M., Popoff, M., Sosson,
449 M., 2000. Crustal strain in the Southern Alps, 1948-1998.
450 *Tectonophysics*, 319, 1–17.
- 451 Carbon, D., 1996. Pré-étude des indices de déformation
452 récente des chaînons provençaux ayant une relation
453 structurale avec la Faille de la Durance, volume Rep.

- 454 GTR/CEA/1096-60. GEOTER Eds, Clapiers, France.
- 455 Chapman, C., Powell, C.A., Vlahovic, G., Sibol, M.S., 1997.
- 456 A statistical analysis of earthquake focal mechanisms and
457 epicenter locations in the eastern Tennessee seismic zone.
458 Bull. seism. Soc. Am., 87, 1522–1536.
- 459 Combes, P., 1984. La tectonique récente de la Provence oc-
460 cidentale: microtectonique, caractéristiques dynamiques et
461 cinématiques; méthodologie de zonation tectonique et re-
462 lation avec la sismicité. Ph.D. Thesis, University of Stras-
463 bourg, Strasbourg, 182 pp.
- 464 Combes, P., Carbon, D., Cushing, M., Granier, T., Vaskou,
465 P., 1993. Mise en évidence d'un paléoséisme pléistocène
466 supérieur dans la vallée du Rhône: implications sur les con-
467 naissances de la sismicité de la France. C. R. Acad. Sci.
468 Paris, 317, 689–696.
- 469 Cushing, E.M., Bellier, O., Nechtschein, S., Sébrier, M.,
470 Volant, P., Lomax, A., Dervin, P., Guignard, P., Bove, L.,
471 2007. Characterizing seismic activity, 3D geometry, seg-
472 mentation for seismic hazard assessment of a low rate ac-
473 tive fault: the example of the Middle Durance Fault System
474 (SE France). *Geophys. J. Int.* *accepted* .
- 475 Cushing, M., Volant, P., Bellier, O., Sébrier, M., Barroux, E.,
476 Grellet, B., Combes, P., Rosique, T., 1997. A multidisci-
477 plinary experiment to characterize an active fault system
478 in moderate seismic activity area: the example of the Du-
479 rance fault (Southeastern France). *Annales Geophysicae*,
480 15, 233.

- 481 Dietz, L.D., Ellsworth, W.L., 1997. Aftershocks of the Loma
482 Prieta earthquake and their tectonic implications. In: P.A.
483 Reasenber, ed., The Loma Prieta, California, Earthquake
484 of October 17, 1989-Aftershocks and Postseismic Effects,
485 U. S. Geological Survey Professional Paper 1550-D, pp. D5–
486 D47.
- 487 Dubois, P., 1966. Sur la sédimentation et la tectonique du
488 Miocène de la Provence occidentale. Bull. Soc. géol. France,
489 pp. 793–801.
- 490 Fehler, M., House, L., Kaieda, H., 1987. Determining planes
491 along which earthquakes occur: Method and application
492 to earthquake accompanying hydraulic fracturing. J. Geo-
493 phys. Res., 92, 9407–9414.
- 494 Fourniguet, J., 1987. Géodynamique actuelle en France. Une
495 illustration de l'apport des comparaisons de nivellements a
496 l'étude des déformations actuelles. Géochronique, 23, 17–
497 21.
- 498 Frohlich, C., Davis, S.D., 1990. Single-link cluster analysis
499 as a method to evaluate spatial and temporal properties of
500 earthquake catalogues. Geophys. J. Int., 100, 19–32.
- 501 Gaillot, P., Darrozes, J., Courjault-Radé, P., Amorèse,
502 D., 2002. Structural analysis of hypocentral distri-
503 bution of an earthquake sequence using anisotropic
504 wavelets: Method and application. J. Geophys. Res., 107.
505 Doi:10.1029/2001JB000212.
- 506 Ghafiri, A., 1995. Paléosismicité de failles actives en con-
507 texte de sismicité modérée : application à l'évaluation de

- 508 l'aléa sismique dans le Sud-est de la France. Ph.D. Thesis,
509 University of Paris-Sud, France.
- 510 Grellet, B., Combes, P., Granier, T., Philip, H., 1993. Sis-
511 motectonique de la France métropolitaine dans son cadre
512 géologique et géophysique, IPSN, GEO-TER, Université de
513 Montpellier II, IPG Strasbourg. *Mém Soc. géol Fr.*, 164(1),
514 76 pp.
- 515 Kagan, Y., Knopoff, L., 1981. Stochastic synthesis of earth-
516 quake catalogues. *J. Geophys. Res.*, 86, 2853–2862.
- 517 Lacassin, R., Meyer, B., Benedetti, L., Armijo, R., Tappon-
518 nier, P., 1998. Signature morphologique de l'activité de la
519 faille des Cévennes (Languedoc, France). *C. R. Acad. Sci.*
520 *Paris*, 326, 807–815.
- 521 Lacassin, R., Tapponnier, P., Meyer, B., Armijo, R., 2001.
522 Was the Trévaresse thrust the source of the 1909 Lambesc
523 (Provence, France) earthquake ? Historical and geomorphic
524 evidence. *C. R. Acad. Sci. Paris*, 333, 571–581.
- 525 Lambert, J., Levret-Albaret, A., Cushing, M., Durouchoux,
526 C., 1996. *Mille Ans de Séismes en France*. Ouest Editions,
527 Nantes, 84 pp.
- 528 Levret, A., Cushing, M., Peyridieu, G., 1996. Etude des Car-
529 actéristiques de Séismes Historiques en France, Atlas de
530 140 Cartes Macrosismiques. Institut de Protection et de
531 Sûreté Nucléaire, Fontenay-Aux-Roses, 399 pp.
- 532 Levret, A., Loup, C., Goula, X., 1986. The Provence earth-
533 quake of 11th June 1909 (France). A new assessment of
534 near field effects. 8th European Conference on Earthquake

- 535 Engineering, Lisbon, 7-12 September.
- 536 Mattauer, M., 2002. Commentaire sur l'article 'Mouvement
537 post-messinien sur la faille de Nîmes : implications pour la
538 sismotectonique de Provence' par A. Schlupp, G. Clauzon,
539 J.-P. Avouac. Bull. Soc. géol. France, 173, 596–597.
- 540 Molliex, S., Bellier, O., Clauzon, G., Siame, L., Hollender, F.,
541 2007. Miocene to present tectonics and associated morpho-
542 logical responses in a slow deformation domain (Provence,
543 SE France). EGU General Assembly, Vienna, Austria, 15-
544 20 April.
- 545 Nocquet, J.M., 2002. Mesure de la déformation crustale en
546 Europe occidentale par géodésie spatiale. Ph.D. Thesis,
547 University of Nice-Sophia-Antipolis, France.
- 548 Nocquet, J.M., Calais, E., 2004. Geodetic Measurements of
549 Crustal Deformation in the Western Mediterranean and
550 Europe. Pure and Applied Geophysics, 161(3), 661–681.
- 551 Peulvast, J.P., Baroux, E., Bellier, O., Sébrier, M., 1999.
552 Le problème de l'activité des failles de Nîmes, de Salon-
553 Cavaillon et de la Moyenne Durance (SE de la France): ap-
554 ports de la géomorphologie structurale. Géomorphologie,
555 4, 327–358.
- 556 Rebai, S., Philip, H., Taboada, A., 1992. Modern tectonic
557 stress field in the Mediterranean region: evidence for stress
558 deviations at different scale. Geophys. J. Int., 110, 106–140.
- 559 Richards-Dinger, K., Shearer, P., 2000. Earthquake locations
560 in southern California obtained using source-specific sta-
561 tion terms. J. Geophys. Res., 105, 10939–10960.

- 562 Schlupp, A., Clauzon, G., Avouac, J.P., 2001. Mouvement
563 post-messinien sur la faille de Nîmes: implications pour la
564 sismotectonique de la Provence. *Bull. Soc. géol. France*, 6,
565 697–711.
- 566 Sébrier, M., Bellier, ., Peulvast, J.P., Vergely, P., 1998. Com-
567 mentaire à la note de R. Lacassin et al. 'Signature mor-
568 phologique de l'activité de la faille des Cévennes (Langue-
569 doc, France)'. *C. R. Acad. Sci. Paris*, 327, 855–859.
- 570 Sébrier, M., Ghafiri, A., Blès, J.L., 1997. Paleoseismicity in
571 France: fault trench studies in a region of moderate seis-
572 micity. *J. Geodyn.*, 24, 207–217.
- 573 Suzuki, Z., Suzuki, K., 1965. On space distribution function
574 of earthquakes. *Sci. Rep. Tohoku Univ.*, 5th Ser. Geophys.,
575 17, 9–23.
- 576 Suzuki, Z., Suzuki, K., 1966. Change in spatial distribution of
577 earthquakes against hypocentral depth. *Sci. Rep. Tohoku*
578 *Univ.*, 5th Ser. Geophys., 17, 159–168.
- 579 Tosi, P., Rubeis, V.D., Papadimitriou, E., Dimitriu, P., 1994.
580 Statistical study of epicentre alignments in the broader
581 Aegean area. *Ann. Geofis.*, 37, 939–948.
- 582 Vere-Jones, D., 1978. Space-time correlations for
583 microearthquakes-A pilot study. *Adv. Appl. Probab.*, 10,
584 73–87.
- 585 Volant, P., Berge-Thierry, C., Dervin, P., Cushing, M., Mo-
586 hammadioun, G., Mathieu, F., 2000. The South Eastern
587 Durance Fault Permanent Network: Preliminary results. *J.*
588 *Seism*, 4, 175–189.

- 589 Volant, P., Lomax, A., Nechtschein, S., Cushing, M., Ait-
590 Ettajer, T., Berge-Thierry, C., Dervin, P., 2003. Locali-
591 sation 3D et calcul de magnitude pour les événements du
592 réseau Durance. AFPS 6th national meeting (French As-
593 sociation for Earthquake Engineering), Palaiseau, France,
594 01-03 July.
- 595 Wessel, P., Smith, W.H.F., 1991. Free software helps map
596 and display data. *Eos Trans. AGU*, 72, 445–446.
- 597 Wesson, R.L., Bakun, W.H., Perkins, D.M., 2003. Association
598 of earthquakes and faults in the San Francisco Bay area
599 using Bayesian Inference. *Bull. seism. Soc. Am.*, 93, 1306–
600 1332.

Seismolineament	Blade length and location	p-value
Villefort	35 km	$2.945 \cdot 10^{-6}$
	70 km	$7.075 \cdot 10^{-5}$
Cévennes	35 km	$6.393 \cdot 10^{-3}$
	70 km	$3.156 \cdot 10^{-6}$
Durance	35 km, northern blade	$7.249 \cdot 10^{-3}$
	35 km, central blade	$3.585 \cdot 10^{-3}$
	35 km, southern blade	$10^{-9} <$
	70 km, northern blade	$4.904 \cdot 10^{-3}$
	70 km, southern blade	$3.072 \cdot 10^{-6}$
Salon-Cavaillon	35 km	$3.585 \cdot 10^{-3}$

Table 1

Probabilities of the type I error for each blade of a detected seismolineament. A type I error occurs when one rejects the null hypothesis when it is true. In the Blade Method, the null hypothesis is that the observed number of points in the blade is the result of Bernoulli trials (Amorèse et al., 1999).

Fig. 1. Tectonic sketch of the study regions showing (A) historical (Lambert et al., 1996) and (B) instrumental (LDG-CEA, 1962-2005) seismicity. Five seismicity clusters (sc1, sc2, sc3, sc4, sc5) are visible in the present seismicity. The abbreviation SCFS stands for Salon-Cavaillon Fault System, Hte Prov. corresponds to Haute Provence, Ch.-du-Pape stands for Châteauneuf-du-Pape. Faults are drawn from the seismotectonic map of France at 1/1 000 000 (Grellet et al., 1993)

Fig. 2. Explanatory sketch of the Blade method. Each point is an epicenter. An incrementally rotating blade (dashed line) is investigating a circular zone (dotted line) around each epicenter. The number of epicenters inside each blade is counted and compared with the number of epicenters inside the disk.

Fig. 3. The length distribution of regional faults in the study regions. The faults used to draw this diagram are those displayed in Figure 1.

Fig. 4. Maps showing the $M \geq 1.0$ seismicity in the 1989 Loma Prieta earthquake region before the mainshock occurrence (January 1, 1979, through October 17, 1989). Data are from the Northern California Earthquake Catalog. Star marks the epicenter of the $M_s=7.1$ mainshock initiated at 00:04:15.28 UTC on October 18, 1989 (Dietz and Ellsworth, 1997). a) Epicenters of all the $M \geq 1.0$ events (8770) and b) epicenters of the best $M \geq 1.0$ located events (4174). The selected hypocenters have root mean square residual (RMS) < 0.1 s, number of P and S times with final weights greater than $0.1 \geq 24$, horizontal standard error (ERH) < 1.0 km and vertical standard error (ERZ) < 2.0 km. The maps show that several epicenters fall in the area around the mainshock (star): during the interseismic phase of the earthquake cycle, "aseismicity" is not complete. b) shows the result of the Blade Method (0.01 significance level, 40x4 km blades, 10° wide rotation angular increment) on the best located events. Close to the Loma Prieta mainshock area, the microseismicity distribution is consistent with a NW-SE fault zone: the Blade Method can be successful even during the interseismic phase of the earthquake cycle.

Fig. 5. Map showing the results of the Blade Method applied to the instrumental seismicity of the studied regions. Boxes identify the zones that are zoomed in Figures 6 to 10. Blades are 35 km long and 12 km wide. The small circles are the 873 investigated earthquake pseudo-locations.

Fig. 6. Map showing the results of the Blade Method in the Aubrac plateau area (35 x 12 km blades). The small circles are the earthquake pseudo-locations. Rose diagrams show the strikes of the faults and of the blades.

Fig. 7. Maps showing the results of the Blade Method in the Montélimar area. Blades filled by patterns can be sensibly associated with a known fault (they are close and parallel or sub-parallel to a known fault). Unfilled blades are not easily associable with a previously recognized fault zone. The small circles are the earthquake pseudo-locations. The squares are the historical earthquakes macroseismic epicenters (Lambert et al., 1996). a) 35 x 12 km and b) 70 x 12 km blades.

Fig. 8. Maps showing the results of the Blade Method in the Durance fault area. a) 35 x 12 km and b) 70 x 12 km blades. The focal solutions (lower hemisphere) of two $M_L = 2.9$ seismic events are from Volant et al. (2000). The date is labelled at the solutions (format yymmdd). The rest of the legend is the same as in Figure 7.

Fig. 9. Map showing the results of the Blade Method in the Salon-Cavaillon fault system area (35 x 12 km blades). The rest of the legend is the same as in Figure 7.

Fig. 10. Map showing the results of the Blade Method in the Espinouse mount area (35 x 12 km blades). The small circles are the earthquake pseudo-locations.

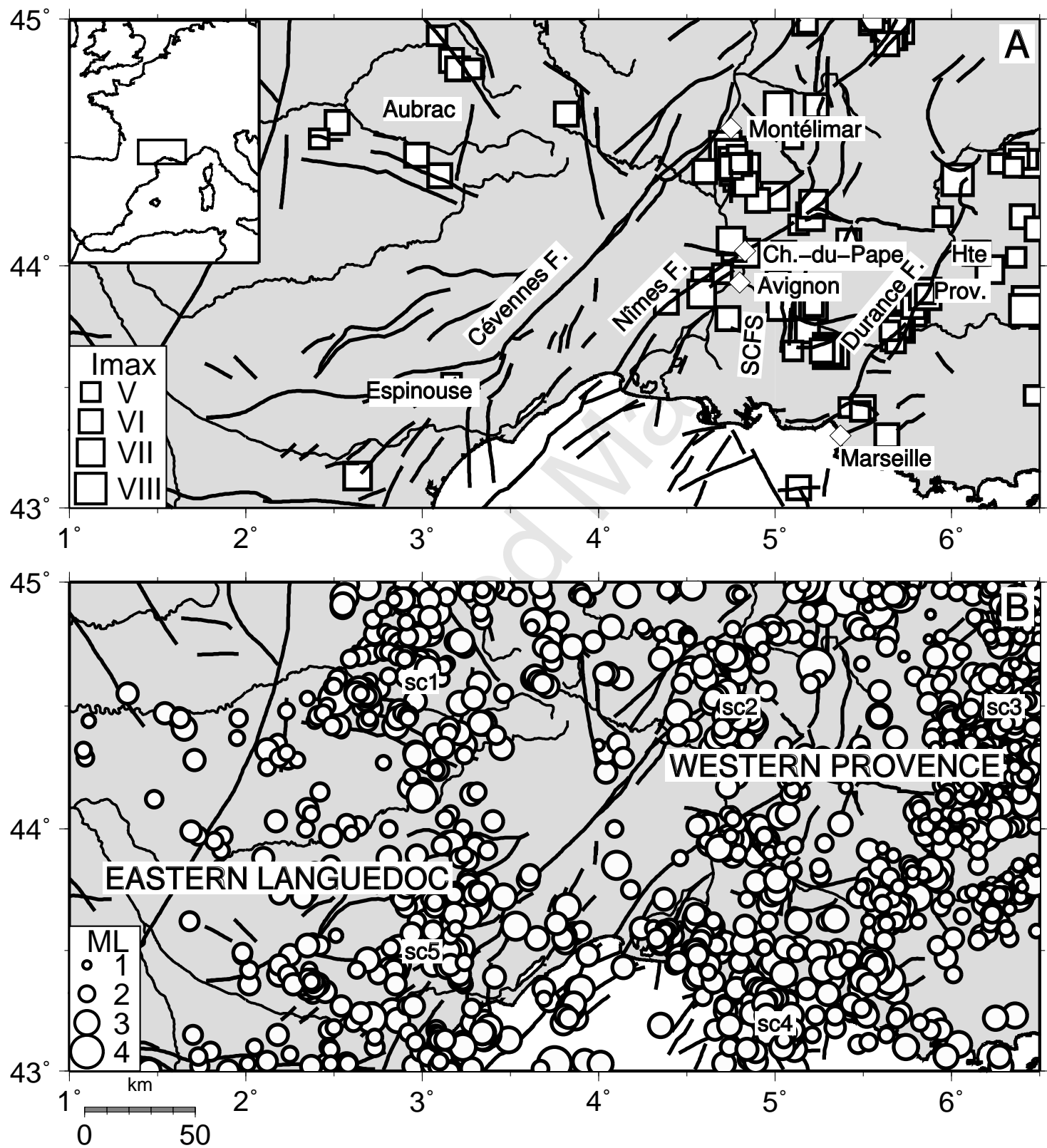


Figure 2, Explanatory sketch

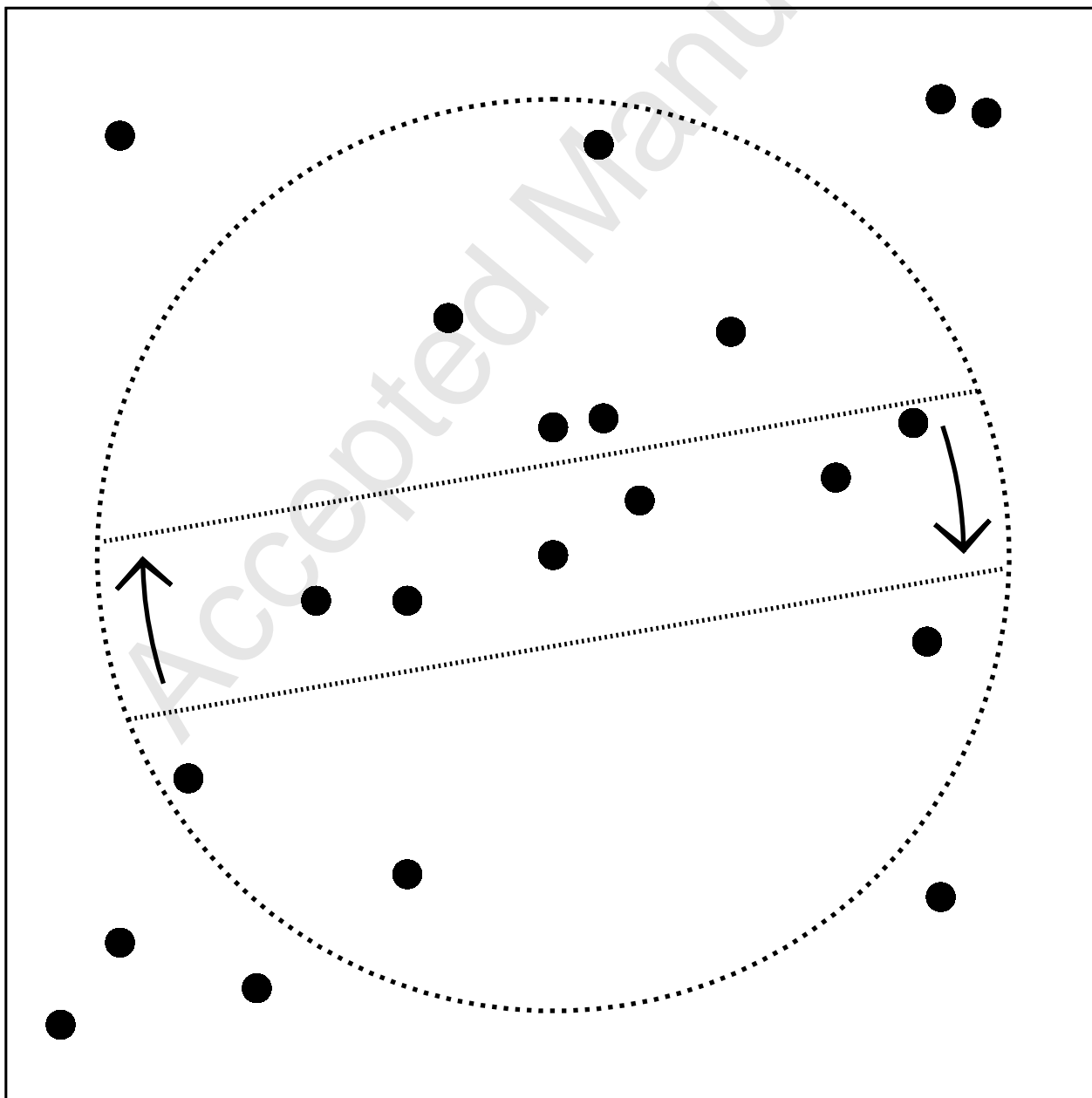


Figure 3, length distribution

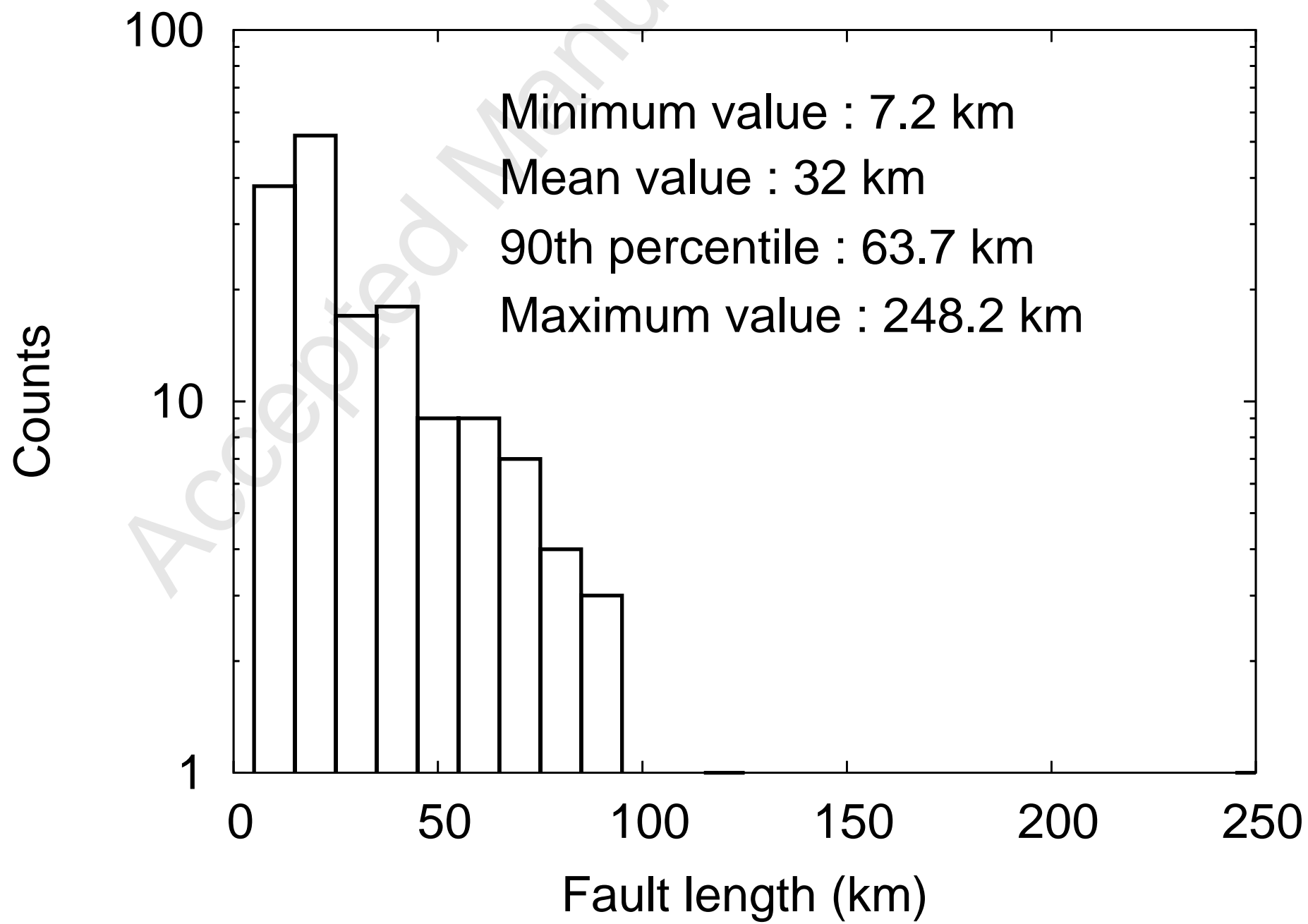
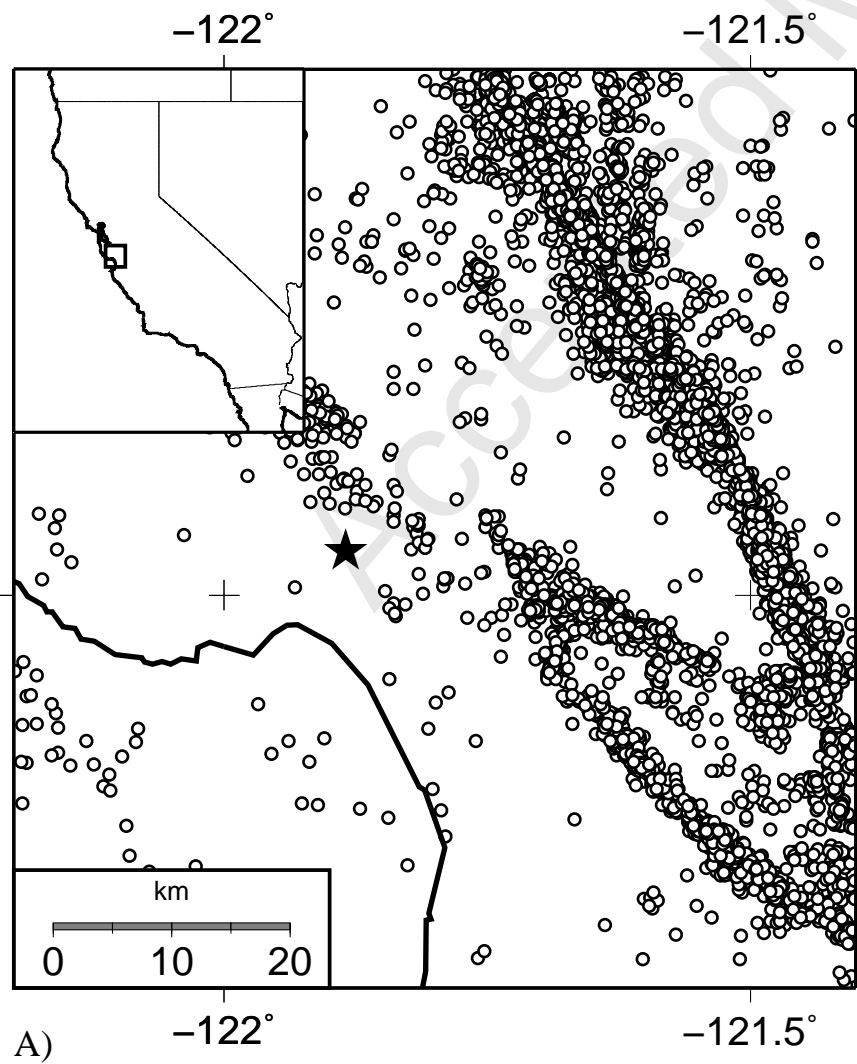
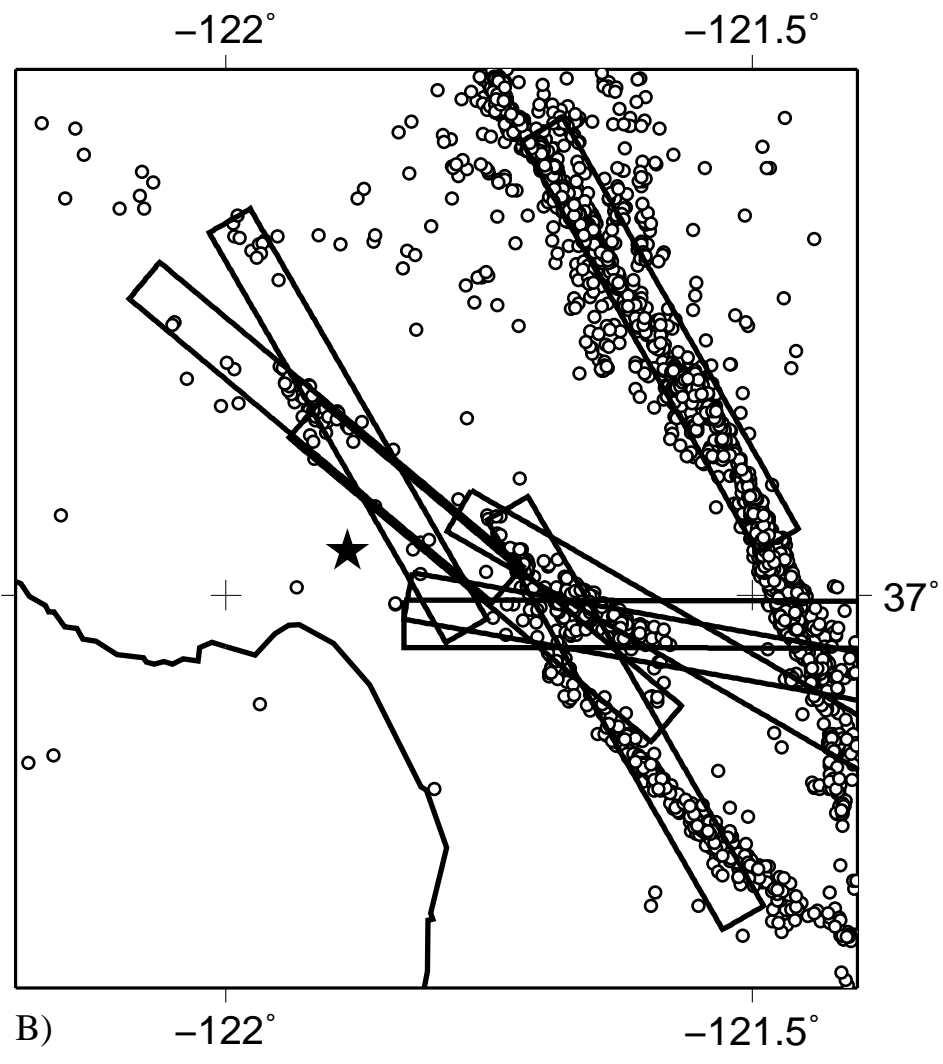


Figure 4. maps California



A) -122° -121.5°



B) -122° -121.5°

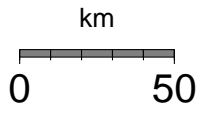
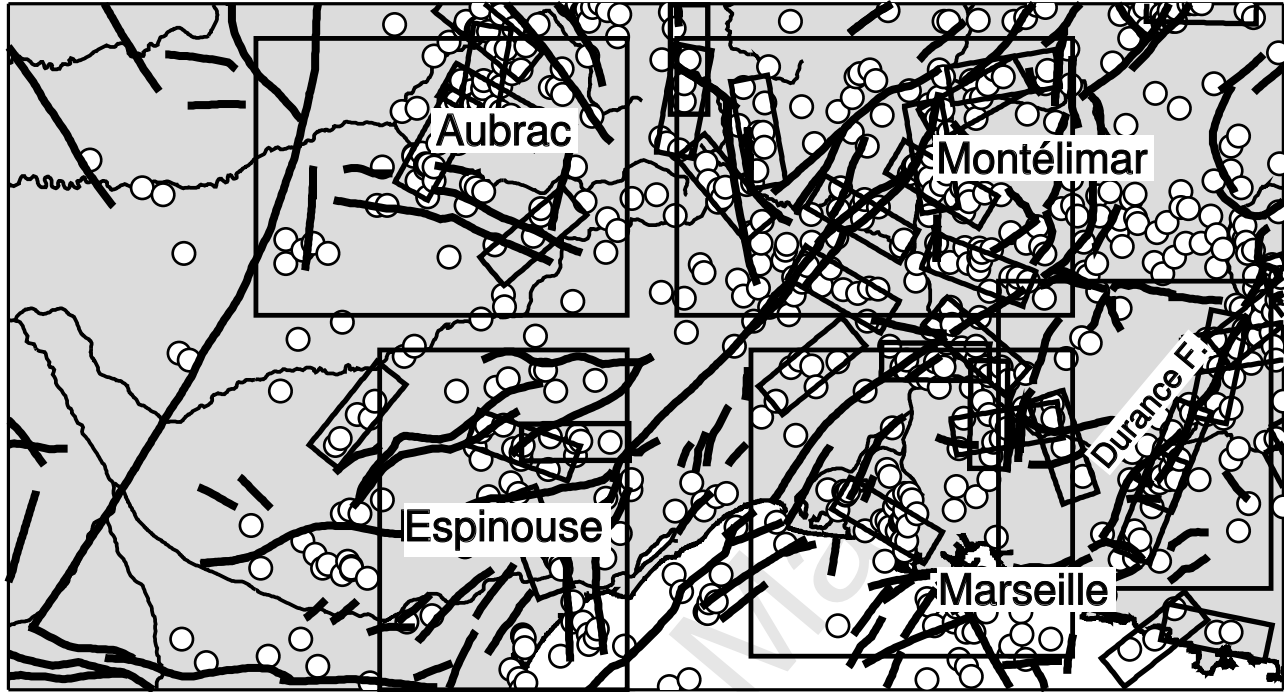


Figure 6. map Aubrac

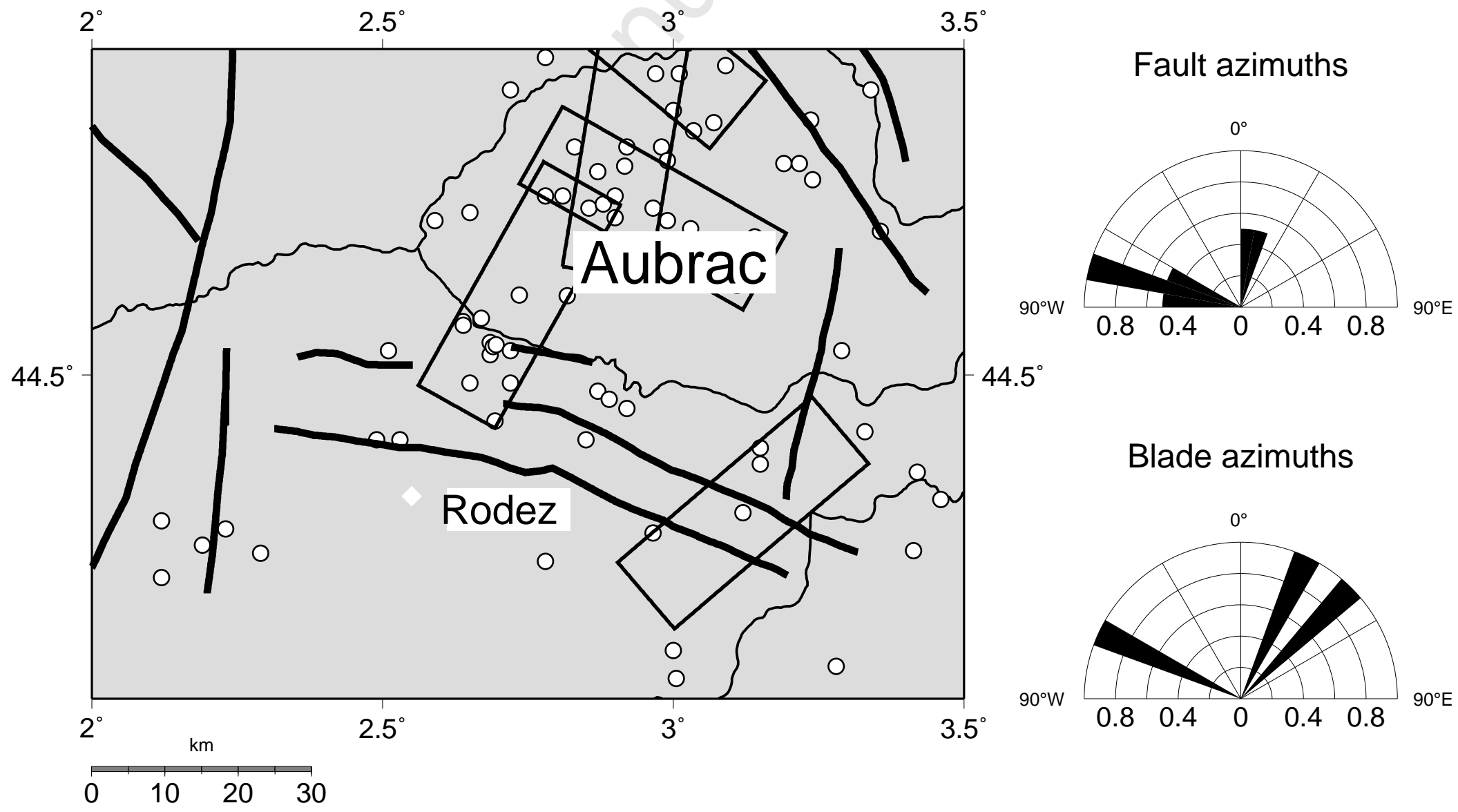


Figure 7. part A map Montelimar

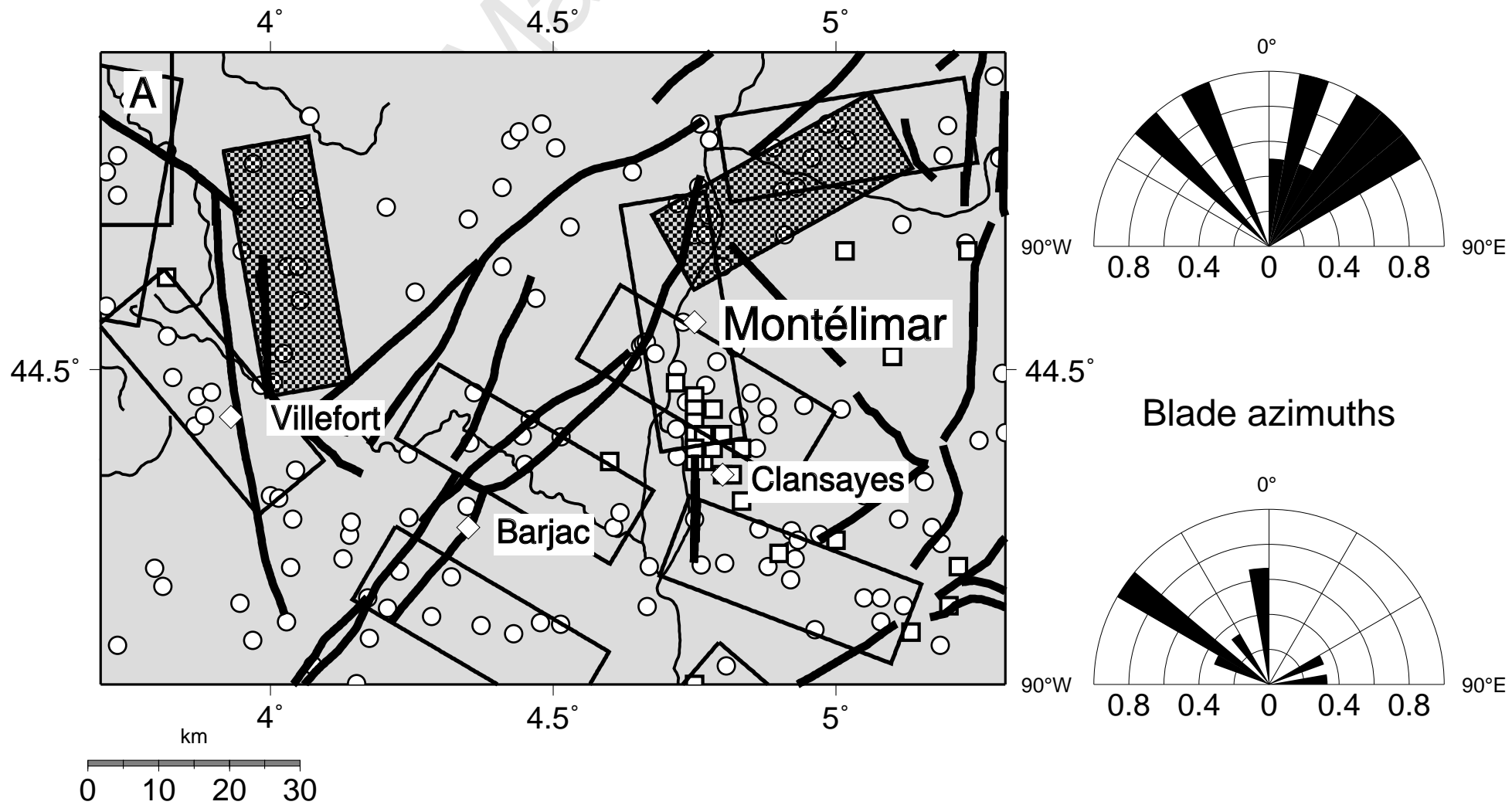


Figure 7. part B map Montelimar

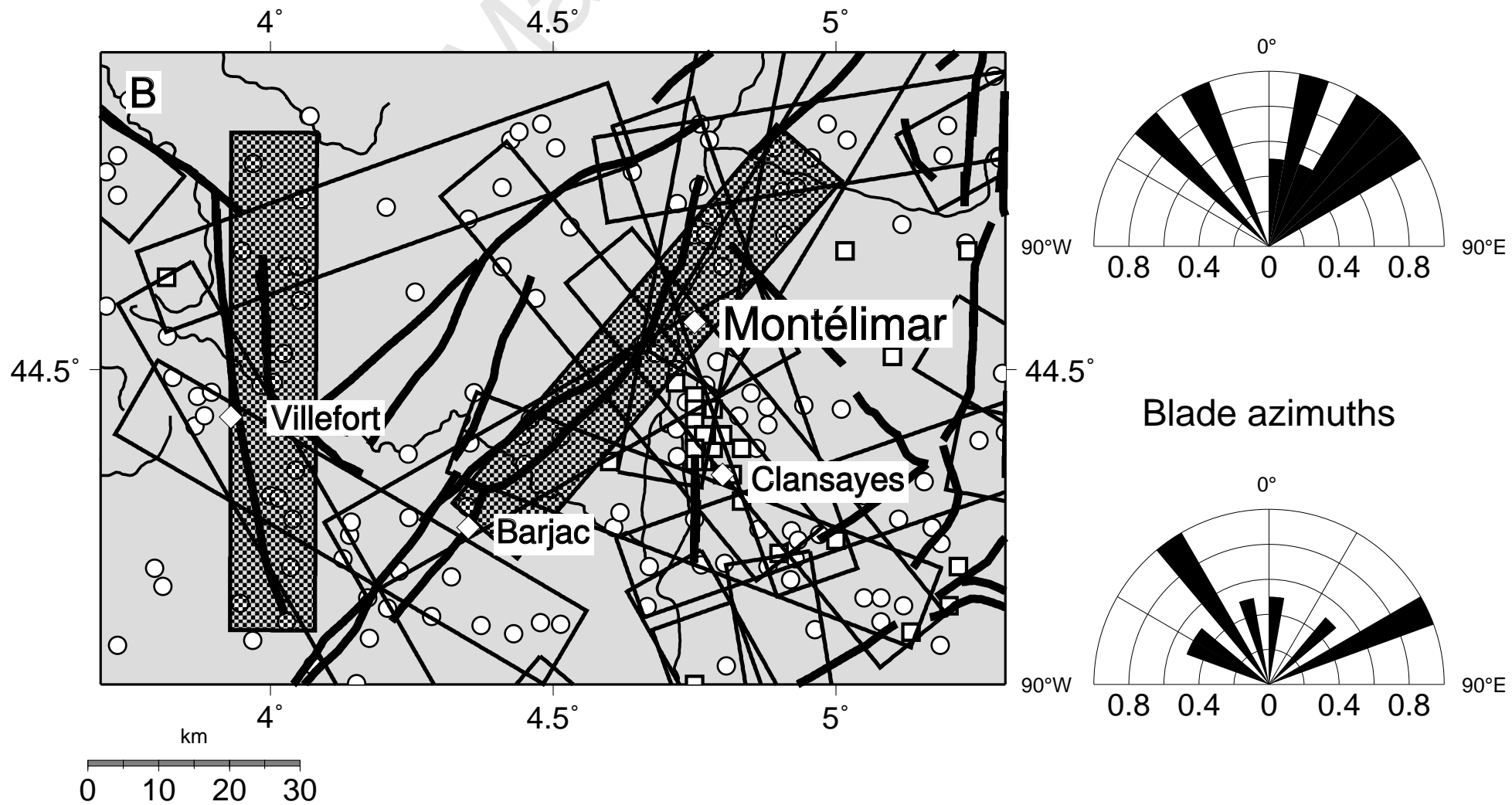
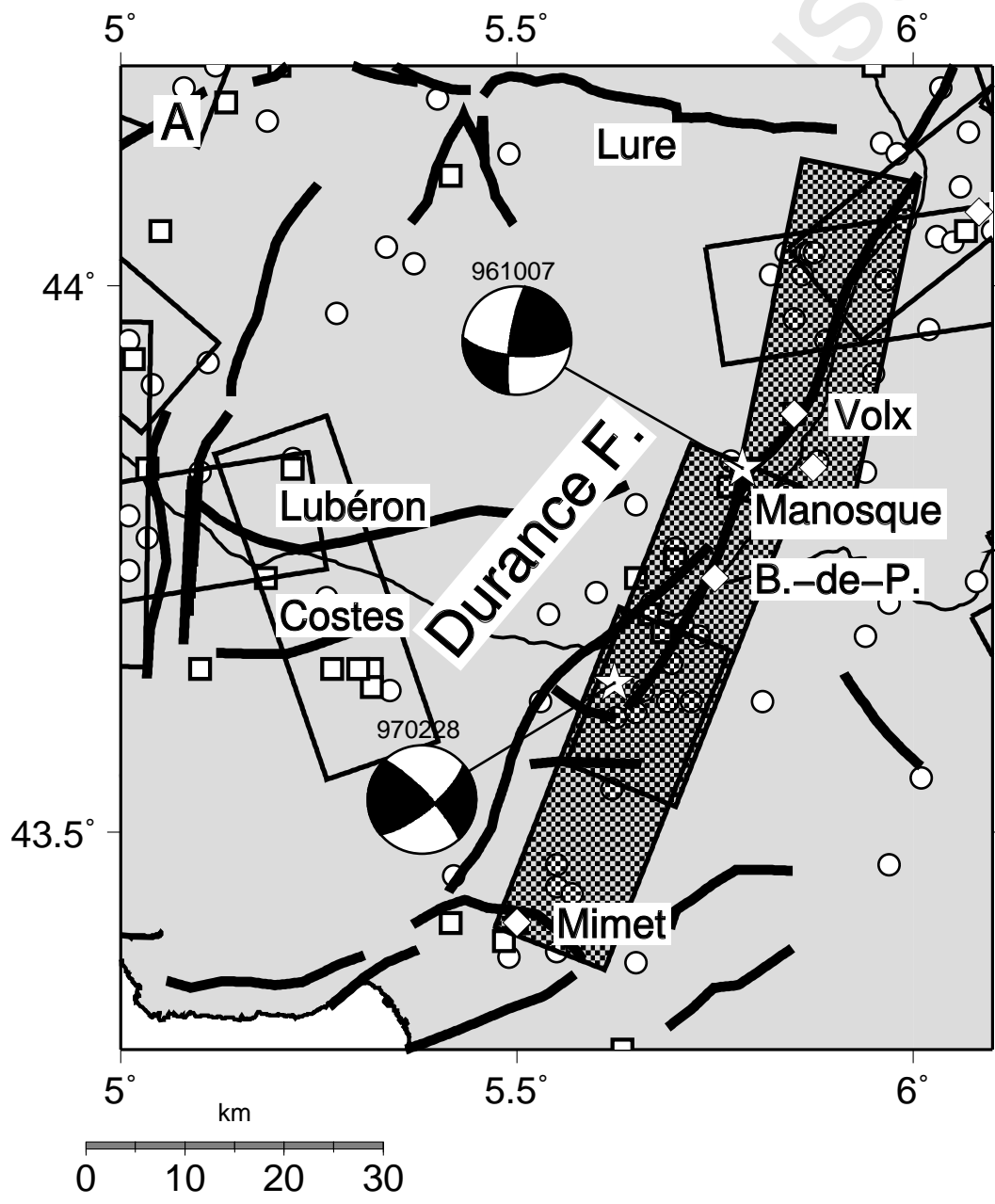
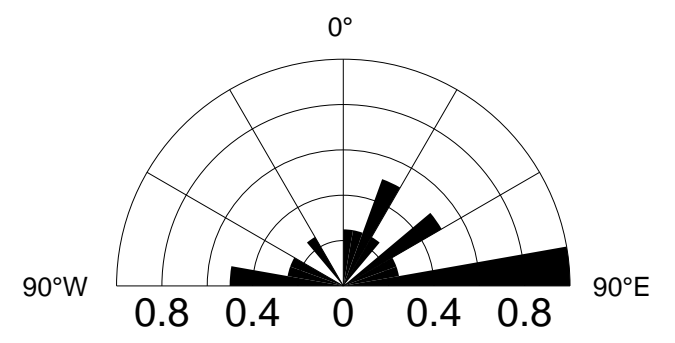


Figure 8. part A map Durance



Fault azimuths



Blade azimuths

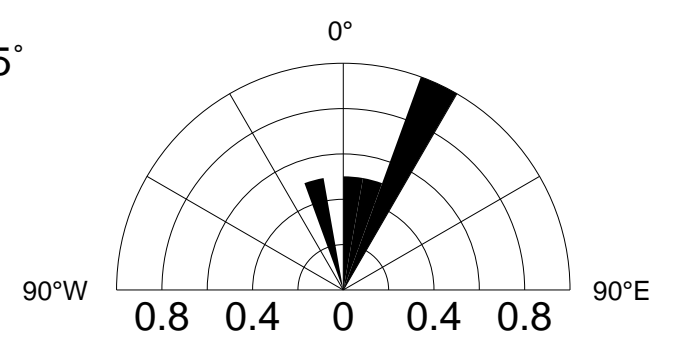
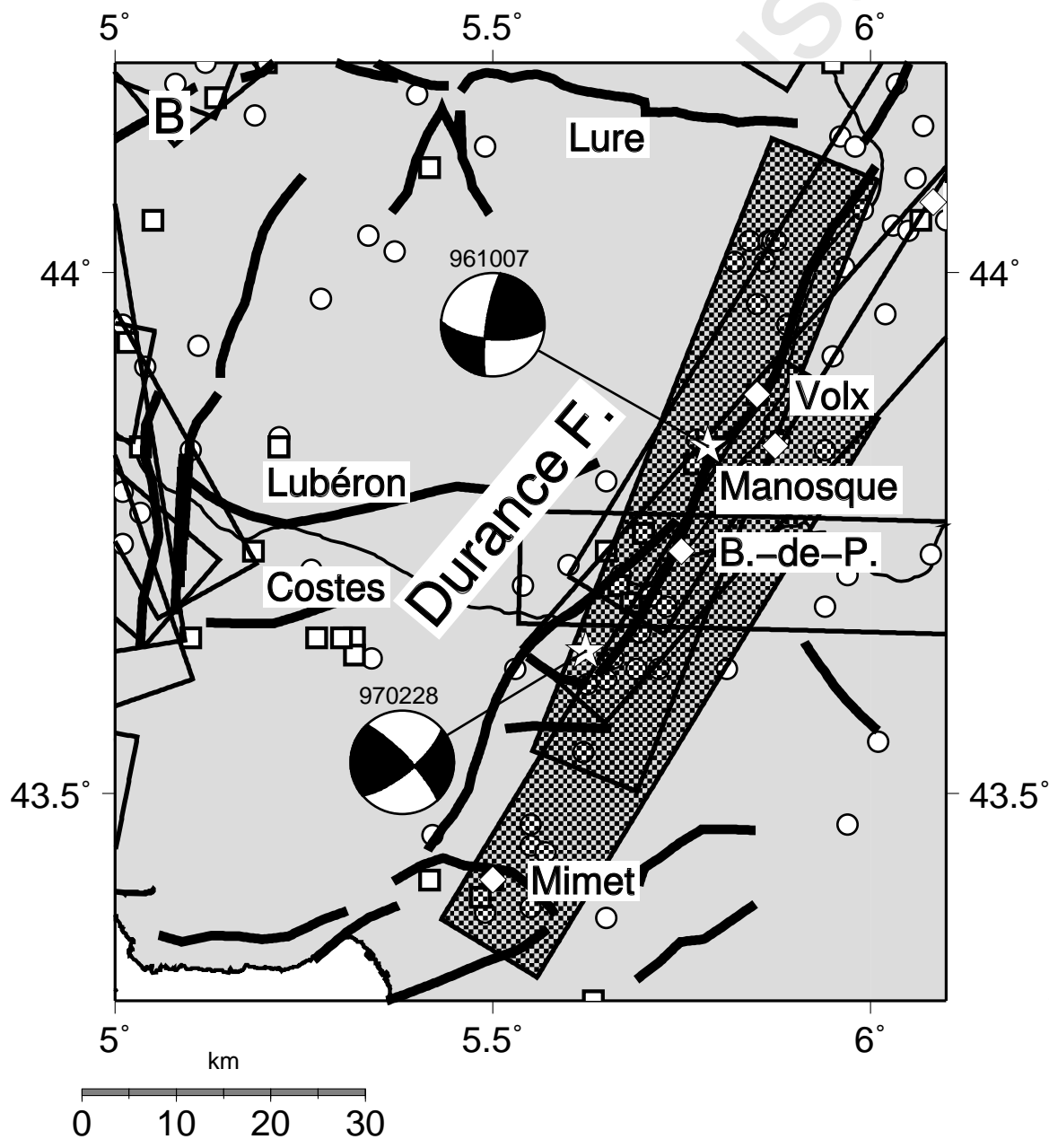
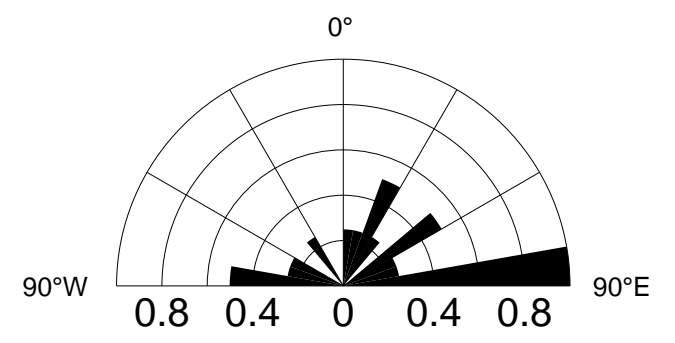


Figure 8. part B map Durance



Fault azimuths



Blade azimuths

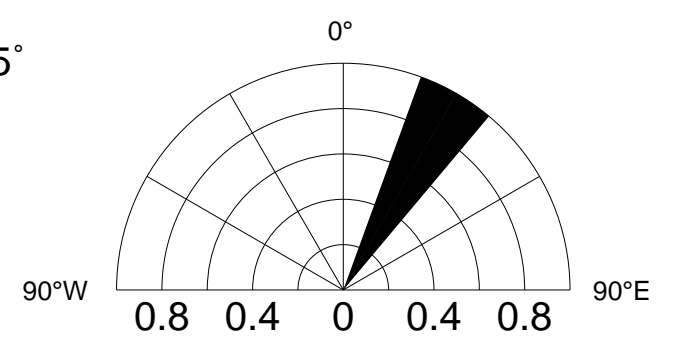
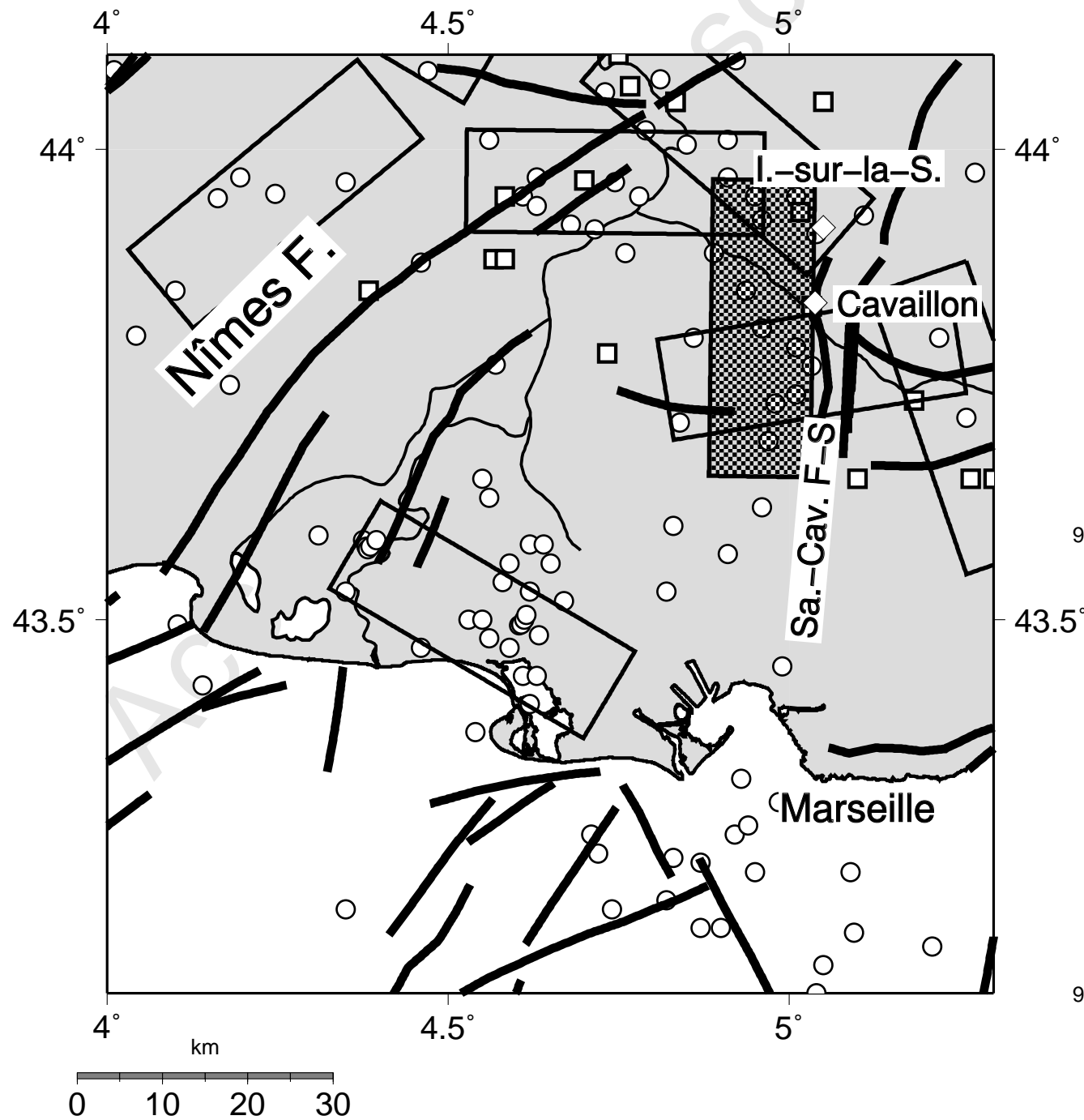
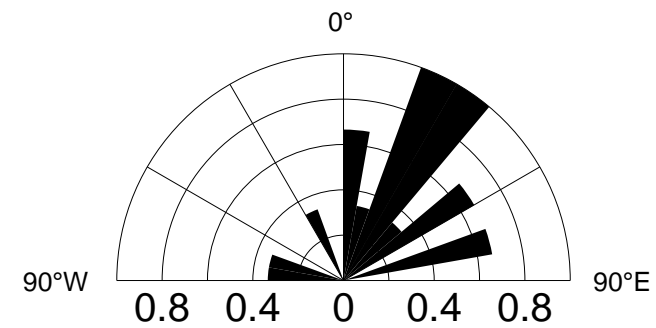


Figure 9. map Salon-Cavaillon



Fault azimuths



Blade azimuths

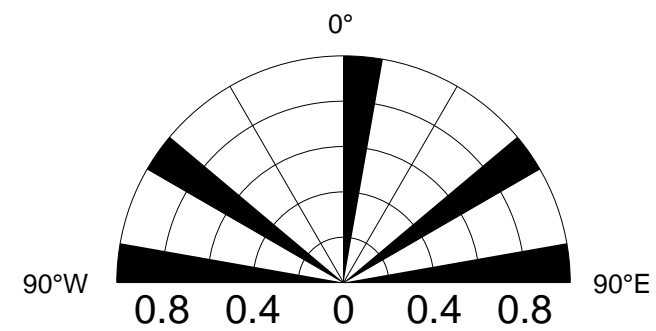


Figure 10. map Espinouse

